

AD-A232 692

DTIC  
REF ID: A62700  
MAR 12 1991

McDonnell Douglas Research  
Laboratories

91 3 06 100

UNCLASSIFIED

SECURITY CLASSIFICATION OF THIS PAGE

## REPORT DOCUMENTATION PAGE

1a. REPORT SECURITY CLASSIFICATION Unclassified		1b. RESTRICTIVE MARKINGS	
2a. SECURITY CLASSIFICATION AUTHORITY		3. DISTRIBUTION/AVAILABILITY OF REPORT Approved for public release; distribution unlimited	
2b. DECLASSIFICATION / DOWNGRADING SCHEDULE			
4. PERFORMING ORGANIZATION REPORT NUMBER(S)		5. MONITORING ORGANIZATION REPORT NUMBER(S)	
6a. NAME OF PERFORMING ORGANIZATION McDonnell Douglas Research Laboratories		6b. OFFICE SYMBOL (If applicable)	7a. NAME OF MONITORING ORGANIZATION AFOSR/NA
6c. ADDRESS (City, State, and ZIP Code) P.O. Box 516 St. Louis, MO 63166		7b. ADDRESS (City, State, and ZIP Code) Bolling Air Force Base Washington, D.C. 20332 BIC 410	
8a. NAME OF FUNDING/SPONSORING ORGANIZATION Department of the Air Force		8b. OFFICE SYMBOL (If applicable) AFOSR/NA	9. PROCUREMENT INSTRUMENT IDENTIFICATION NUMBER F49620-86-C-0090DEF
8c. ADDRESS (City, State, and ZIP Code) Air Force Office of Scientific Research/AFOSR Bolling Air Force Base Washington, DC 20332		10. SOURCE OF FUNDING NUMBERS PROGRAM ELEMENT NO. 6102P PROJECT NO. 2307 TASK NO. A2 WORK UNIT ACCESSION NO. 2	
11. TITLE (Include Security Classification) Vortex System Evolution in 2- and 3-D Swept Trailing Edge Flows			
12. PERSONAL AUTHOR(S) Roos, Frederick W.; Kegelman, Jerome T.; Wlezien, Richard W.; Parekh, David E.; Kibens, Valdis			
13a. TYPE OF REPORT First Technical	13b. TIME COVERED FROM 87 Sep 1 TO 89 Aug 31	14. DATE OF REPORT (Year, Month, Day) 1990 July 24	15. PAGE COUNT 27
16. SUPPLEMENTARY NOTATION			
17. COSATI CODES		18. SUBJECT TERMS (Continue on reverse if necessary and identify by block number) Fluid mechanics Passive control Control of turbulence Shear layers Active control Asymmetric nozzles Jet flows Image processing Slanted nozzles	
19. ABSTRACT (Continue on reverse if necessary and identify by block number) Instability waveform orientation and vortex-system interaction were studied in a swept-trailing-edge mixing layer and in a slanted nozzle jet flowfield at low subsonic velocities. Flow visualization and image processing, and hot-wire data comprised the main body of experimental observations. The response of full-span wave systems of swept and unswept orientation were documented as a function of acoustic excitation introduced through a thin slot at the trailing edge. The lateral spreading of a wave system with only partial-span excitation was shown to be asymmetrical in a swept mixing layer. The jet flowfield was studied using a simultaneous axial and transverse laser-sheet illumination. Excitation frequency- and amplitude-dependence of instability-wave-system orientation was characterized. Digitized flow-visualization images were decomposed to show the axial and helical shear-layer modes.			
20. DISTRIBUTION/AVAILABILITY OF ABSTRACT <input checked="" type="checkbox"/> UNCLASSIFIED/UNLIMITED <input type="checkbox"/> SAME AS RPT. <input type="checkbox"/> DTIC USERS		21. ABSTRACT SECURITY CLASSIFICATION Unclassified	
22a. NAME OF RESPONSIBLE INDIVIDUAL James M. McMichael		22b. TELEPHONE (Include Area Code) (202) 767-4935	22c. OFFICE SYMBOL AFOSR/NA

## Preface

The work reported herein was performed by the McDonnell Douglas Research Laboratories in St. Louis, Missouri, for the United States Air Force Office of Scientific Research, Bolling Air Force Base, Washington, DC, under Contract No. F49620-86-C-0090DEF. The work reported was conducted from 1 September 1987 to 31 August 1989 in the Flight Sciences Department, managed by Dr. R. J. Hakkinen. The principal investigator was Dr. V. Kibens. Co-investigators were Dr. F. W. Roos, Dr. J. T. Kegelman, Dr. R. W. Wlezien, and Dr. D. E. Parekh.

The present report and MDC Report No. QA005, dated 15 January 1988, entitled "Three Dimensional Vortex Interactions," contain the full description of the technical work performed under this contract.

The final technical report has been reviewed and approved.

R. J. Hakkinen

R. J. Hakkinen  
Director-Research, Flight Sciences  
McDonnell Douglas Research Laboratories

J. O. Dimmock

J. O. Dimmock  
Staff Vice President-Research  
McDonnell Douglas Research Laboratories

Accession For	
NTIS	CRA&I <input checked="" type="checkbox"/>
DTIC	TAB <input type="checkbox"/>
Announced	<input type="checkbox"/>
Publication	<input type="checkbox"/>
By	
L. J. Dimmock	
Availability Codes	
Dist	Avail and/or Special
A-1	



## TABLE OF CONTENTS

Section	Page
1. INTRODUCTION.....	1
2. SWEPT TRAILING EDGE FLOWS.....	2
2.1 Symmetrical 45 degree Trailing Edge Flows.....	2
2.2 30 Degree Sweep Trailing Edge.....	4
2.3 Finite Span Waves.....	7
3. EVOLUTION OF VORTEX SYSTEMS IN A CIRCULAR SHEAR LAYER.....	11
3.1 Background.....	11
3.2 Approach.....	13
3.3 Results and Discussion.....	14
4. CONCLUSIONS.....	24
5. REFERENCES.....	26
6. PUBLICATIONS AND PRESENTATIONS.....	27

## 1. INTRODUCTION

Work under the present contract treated development of two- and three-dimensional mixing layers. Complex instability-wave patterns had been observed in jet flows from slanted, stepped, and crenelated nozzles (References 1 and 2). The variety of unique dynamic states observed in these earlier studies led to the formulation of an experimental geometry that isolated some of the three-dimensional processes observed in the indeterminate-origin-nozzle flows. We selected a mixing layer behind a swept trailing edge as a simplification of the flow geometry just downstream of the exit plane of a slanted nozzle.

During the first year of this contract, we conducted an initial exploration of instability-wave development in the laminar mixing layer behind a swept trailing edge. The results showed two distinct, interacting families of instability waves, one parallel to the trailing edge and the other perpendicular to the flow. Acoustic excitation of the mixing layer allowed substantial enhancement of either set of waves, depending on excitation frequency. Wavelengths of the two wave families appeared to be the same.

Also during the first year, we developed and demonstrated a technique for quantitatively processing flow-visualization images obtained from the jet flowfield (References 3 and 4). This technique reconstructed a detailed view of the shear layer from a set of azimuthal cross-sections of the flow. The streamwise evolution of the vorticity centroids as seen in the processed images closely matched the vortex tracks detected by phase-conditioned Laser Doppler Velocimetry (LDV). While LDV provided more resolution further downstream, the flow-visualization technique was close to two orders of magnitude faster.

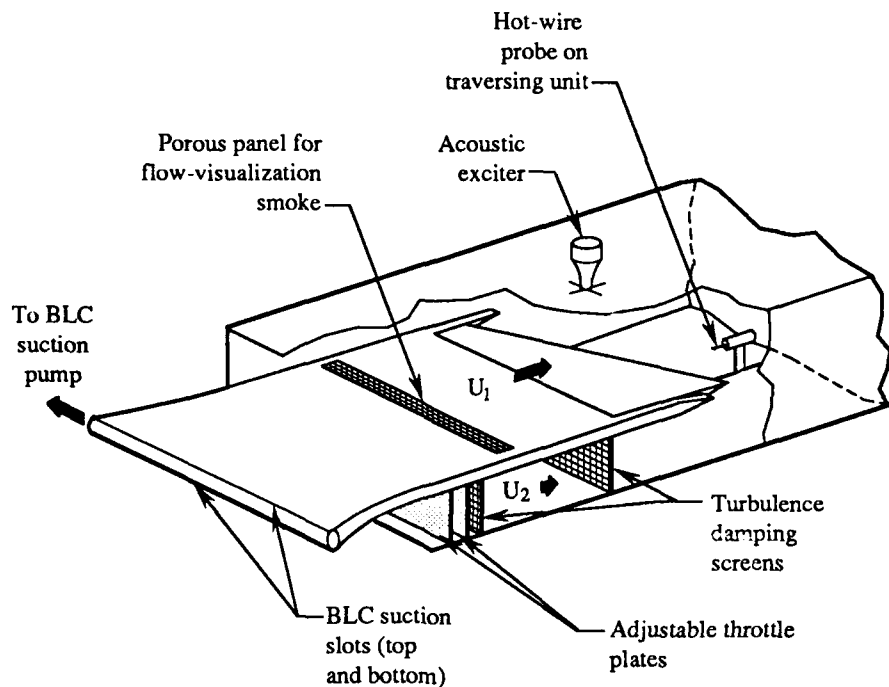
The present report describes the continuation of the work outlined above, conducted in a flow behind a swept trailing edge, and in a jet flowfield exiting from a slanted nozzle.

## 2. SWEPT TRAILING EDGE FLOWS

Experiments on swept trailing edge flows were performed in the MDRL Shear Flow Facility, which is a closed-circuit, low-speed wind tunnel for the study of two-dimensional laminar and turbulent shear layers. The test channel is 0.91 m wide, 0.38 m high, and 5.49 m long, and has an adjustable roof for pressure-gradient control and full-length glass windows for optical access. The flow velocity is controllable from 0.3 to 78 m/s. A two-stream mixing layer flow was generated using the apparatus shown in Figure 1. A splitter plate of 1.27 cm thickness extended from the settling chamber into the test section. Throttling plates and turbulence damping screens provided blockage and flow quality control for the lower stream. Boundary layer suction slots at the leading edge were used to maintain attached flow on both plate surfaces for all flow speeds and speed ratios. The trailing edge of the plates used was symmetrical, with an included angle equal to 5 degrees. A laminar mixing layer was obtained for plate Reynolds numbers up to 1,000,000. Sidewall boundary layers were shown to have no influence on the phenomena studied. A porous panel was used to introduce a polyethylene glycol aerosol ("smoke") into the boundary layer, and a pulsed diffuse-light source was synchronized with excitation frequency to visualize the developing instability wave systems. Weak acoustic excitation was applied from a single source mounted in the ceiling of the test section as shown in Figure 1. Extensive hot-wire surveys were made in the developing mixing layer to quantify the amplitude and phase characteristics of the phenomena observed by flow visualization. The acoustic-excitation signal was used for phase reference. Growth of the excited instability waves was gaged by the excitation-frequency peak in the  $v'$  amplitude spectrum measured at the maximum- $v'$  level of the shear layer at various streamwise and spanwise locations.

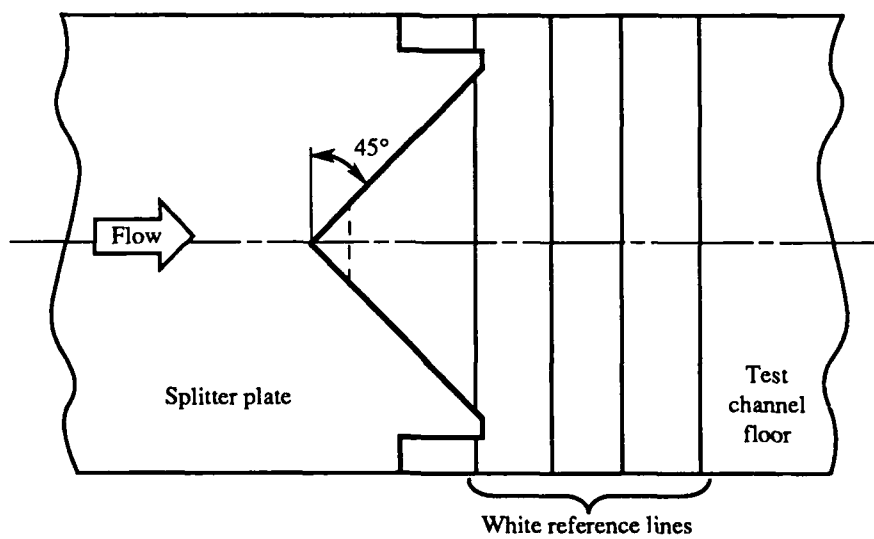
### 2.1 Symmetrical 45 Degree Trailing Edge Flows

A major series of measurements was obtained for a splitter plate geometry indicated in Figure 2, consisting of a symmetrical swept edge arranged in a 'notch' configuration. Results of these experiments are



90-222-541

**Figure 1. Installation sketch showing splitter plate for generating two-stream mixing layer.**



90-222-542a

**Figure 2. Plan view of symmetrical 45°-sweep splitter-plate trailing edge with optional unswept center segment.**

documented in Reference 5. The constant phase lines of the instability waves demonstrated a variety of modal characteristics corresponding to those reported earlier in Reference 3, which showed that instability waves could align either with the sweep angle of the trailing edge, or with the normal to the flow direction. Figure 3 illustrates the extremes of wave alignment, caused by appropriate excitation frequency-changes. (Note that the visualized flow is viewed directly from the side and somewhat above the plane of the mixing layer; the faint "vertical" stripes in the dark background are actually the reference lines noted in Figure 2.) Results were also obtained for a notch arrangement with an unswept center portion, identified by dotted line in Figure 2. Constant-phase and constant-amplitude lines for the two cases of Figure 3 are shown in Figure 4. Streamwise growth of the disturbances varies greatly with spanwise position. The constant phase lines for the two cases confirm the qualitative difference observed visually and the swept/unswept wavelength identity discussed in Reference 3. The flows behind plates with unswept central segments show similar behavior to that in Figure 4. Momentum-thickness growth data are shown in Figure 5.

## 2.2 30 Degree Sweep Trailing Edge

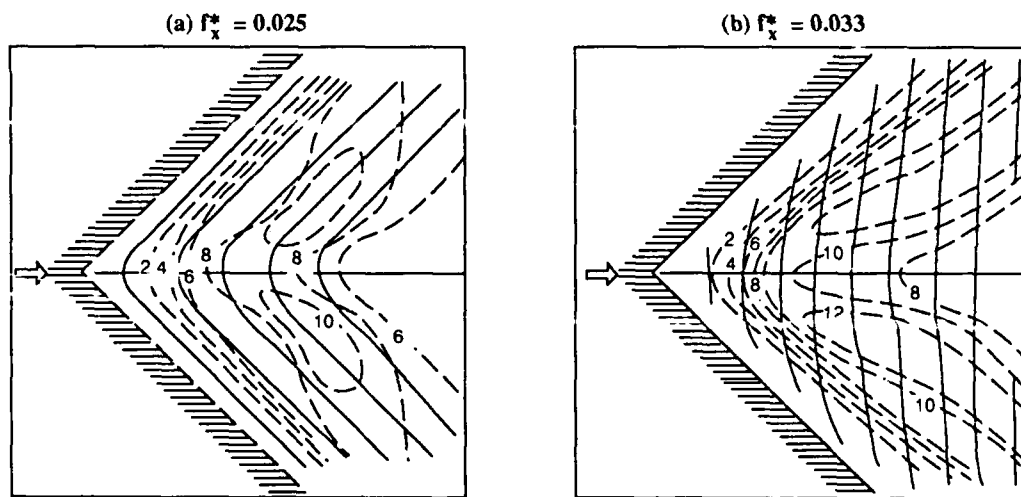
Measurements using a 30 and 45 degree swept edge spanning the entire test section were also taken. Some of these measurements were reported in Reference 3. The 30 degree case illustrated an intermediate wave resolution mode, characterized by a "crossover" phenomenon. As excitation frequency was increased, the initially swept waves gradually oriented themselves at increasingly larger angles with respect to the trailing edge. The increases in this angle occurred through spanwise-localized zones of phase distortion, in which each swept wave appeared to lose spanwise coherence and then reconnect with its up- or downstream neighbor such that the emerging spanwise-coherent wave had reduced sweep.

The 30 degree geometry was also used for studies of spanwise-segmented excitation. Channels internal to the plate trailing edge conducted acoustic waves to five contiguous, separate, narrow exit slots on the upper surface of the plate, spanning the width of, and parallel to, the trailing edge.



90-222-543

**Figure 3. Visualization of instability-wave development downstream of a symmetrical 45°-sweep trailing edge ( $U_1 = 6.2 \text{ m/s}$ ;  $U_1/U_2 = 2.6$ ).**



**Notes:**

— = constant phase ( $2\pi$  increments)

- - - = constant amplitude (relative levels noted)

(All excitation at same amplitude)

90-222-544

**Figure 4. Constant-phase and constant-amplitude contours for various excitation frequencies ( $U_1 = 6.1 \text{ m/s}$ ;  $U_1/U_2 = 2.6$ ).**

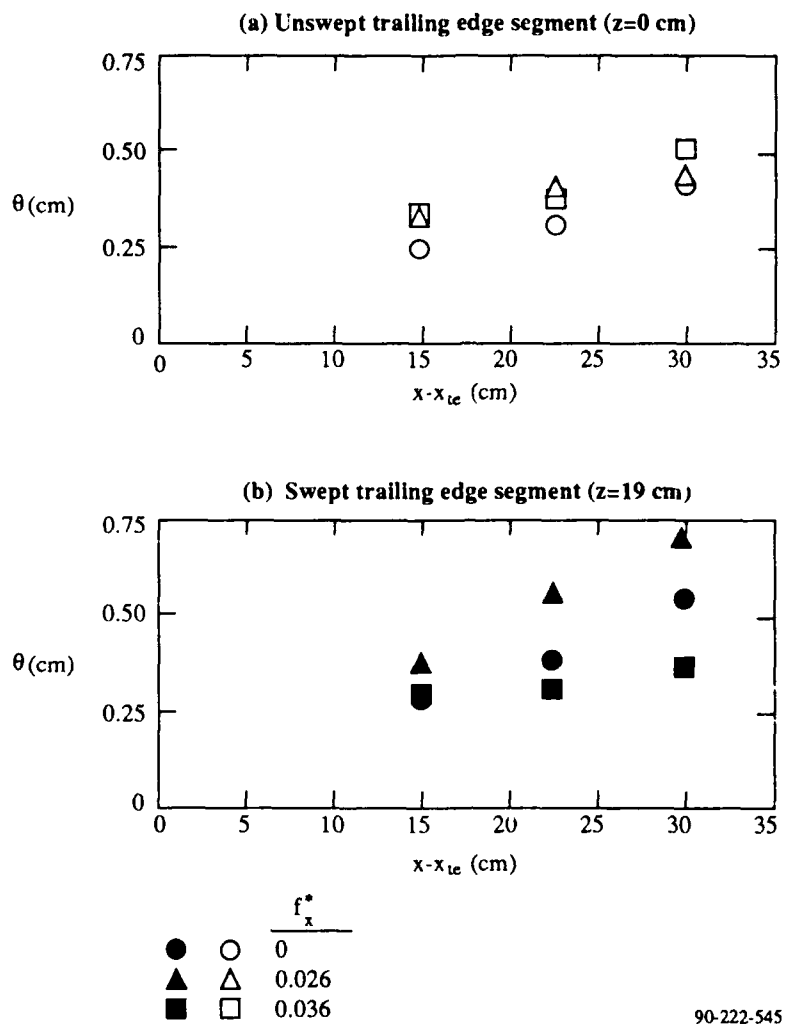


**Figure 5. Momentum-thickness growth downstream of symmetrical-sweep trailing edge with unswept center segment ( $U_1 = 6.1$  m/s;  $U_1/U_2 = 2.6$ ).**

The exit slots were 3 mm wide, and were located 3 mm upstream of the trailing edge.

### 2.3 Finite Span Waves

Experiments were performed exploring the spreading of instability-wave systems of finite span, using only the center segment of the acoustic-excitation system described in the previous section. Detailed results of these tests are documented in Reference 6. The finite-span acoustic slot was located immediately upstream of, and parallel to, the unswept and swept (30 degree) trailing edges. Again, smoke flow-visualization of the viscous layer and extensive hot-wire measurements were employed to characterize the vortex-rollup and wave-spreading phenomena. The unswept case is illustrated in Figure 6. Flow visualization and phase/amplitude evolution indicate that the excited segment of the shear layer is largely confined to the region directly downstream of the excitation slot, and is spreading gradually (and symmetrically) in the lateral direction. The fundamentally convective character of the mixing-layer vortical-structure processes is confirmed by Figure 7, which shows that instability-wave growth downstream of the center excitation slot is insensitive to the presence or absence of excitation from the rest of the slot system. Figure 8 shows how the hot-wire results were used to define the spreading of the finite-span wave system. The sensitivity of lateral spreading to excitation frequency and amplitude, as well as the speed ratio of the two streams, is shown in Figure 9. The spreading characteristics for swept trailing edge, shown in Figure 10, display a lateral asymmetry. Considerable variation with frequency is observed for the lateral spreading of an excited segment of the shear layer, as shown in Figure 11.

(a) Flow visualization



(b) Phase and amplitude of fundamental

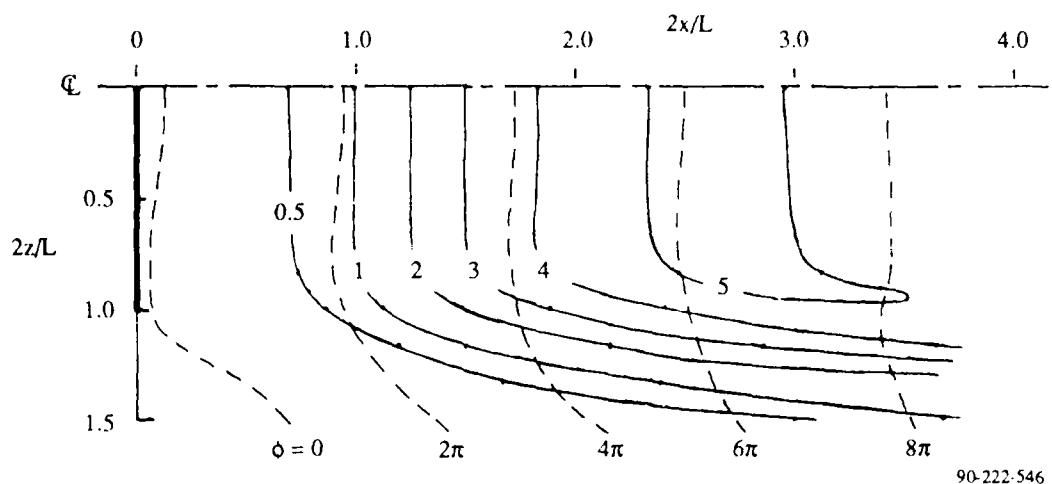


Figure 6. Visualization (a) and corresponding phase/amplitude map (b) of finite-span instability-wave growth downstream of unswept trailing edge (low-amplitude excitation @  $f_x^* = 0.023$ ;  $U_1 = 5.9$  m/s;  $U_1/U_2 = 2.7$ ).

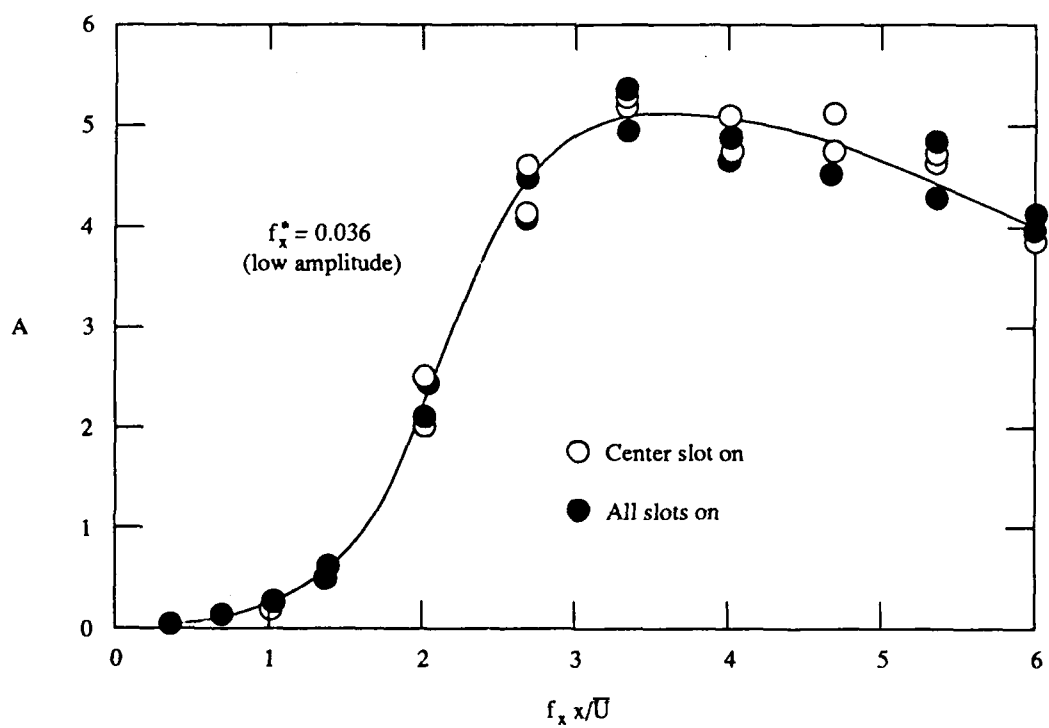
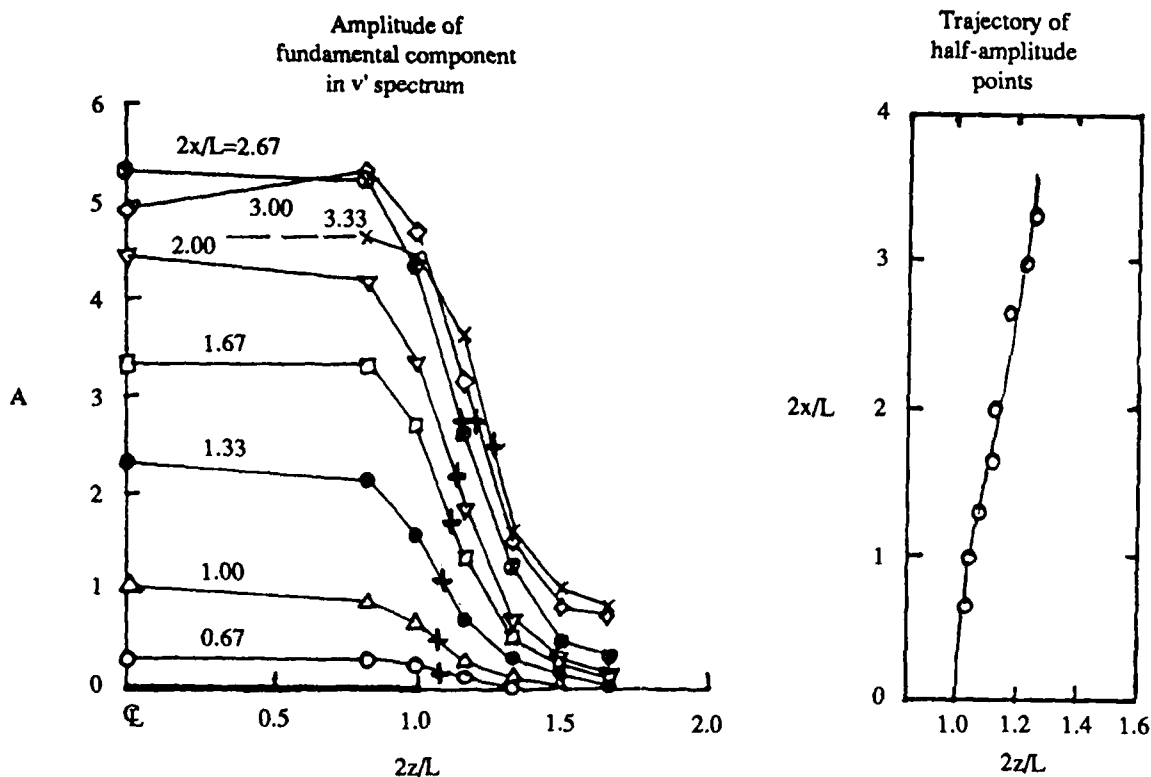
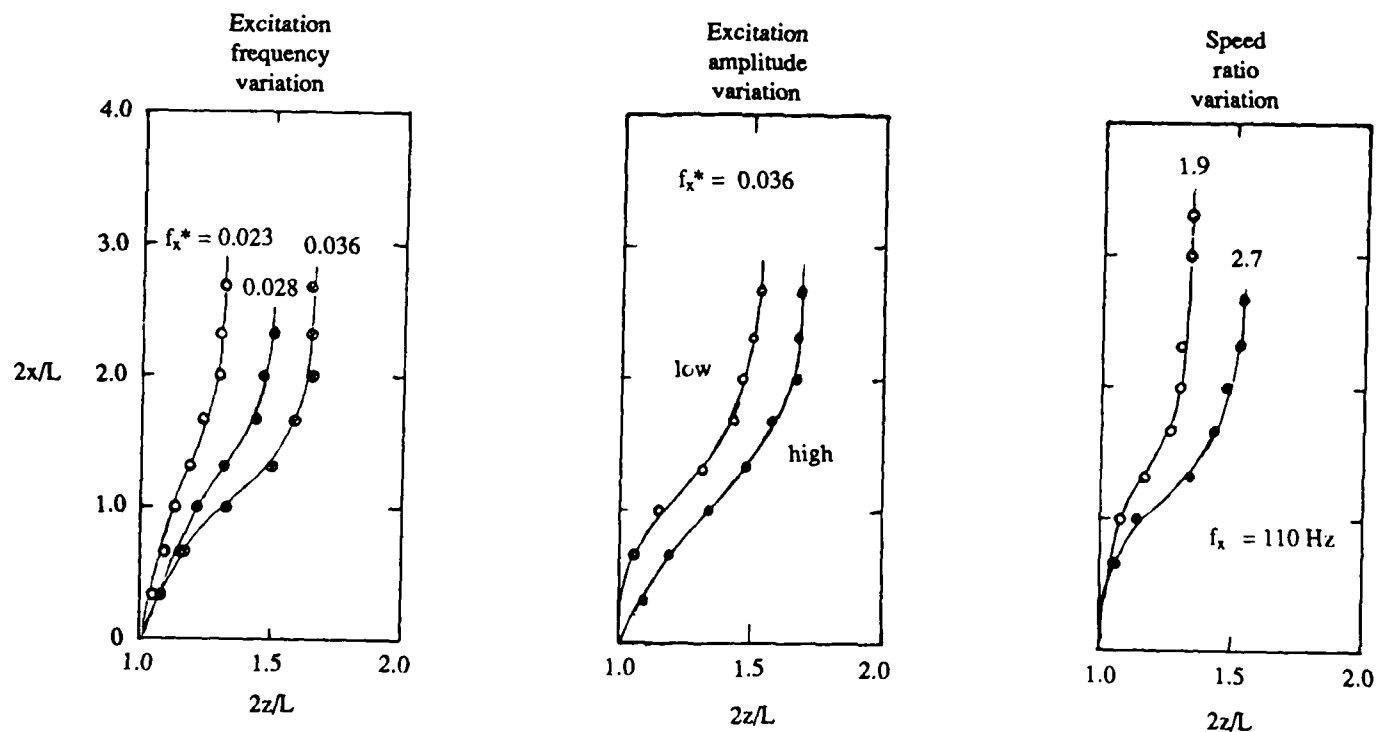


Figure 7. Growth of instability waves downstream of center excitation slot for typical conditions.



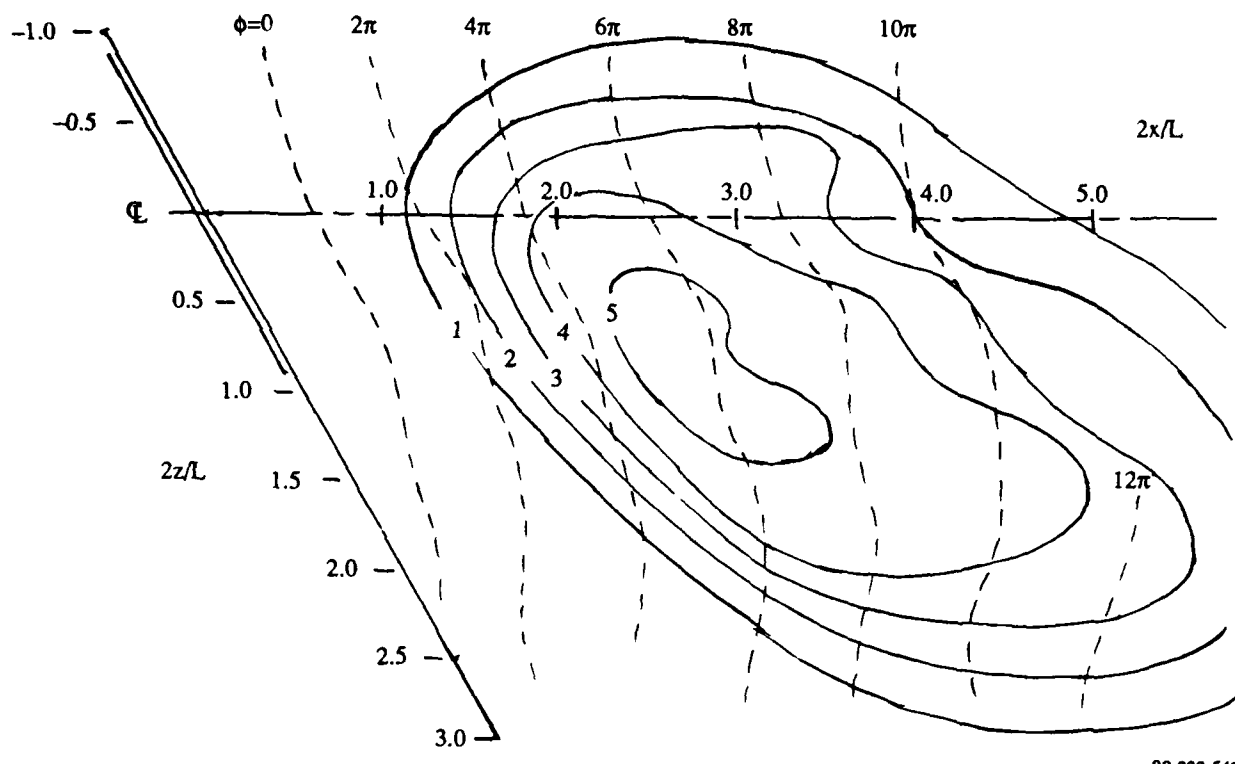
90-222-547

Figure 8. Definition of lateral spreading of finite-span instability waves for conditions of Figure 6.



90-222-548

Figure 9. Sensitivity of lateral spreading to variations in flow and excitation conditions.



**Figure 10. Phase/amplitude map of finite-span instability-wave growth downstream of 30°-sweep trailing edge (low-amplitude excitation @  $f_x^* = 0.036$ ;  $U_1 = 5.9$  m/s;  $U_1/U_2 = 2.7$ ).**

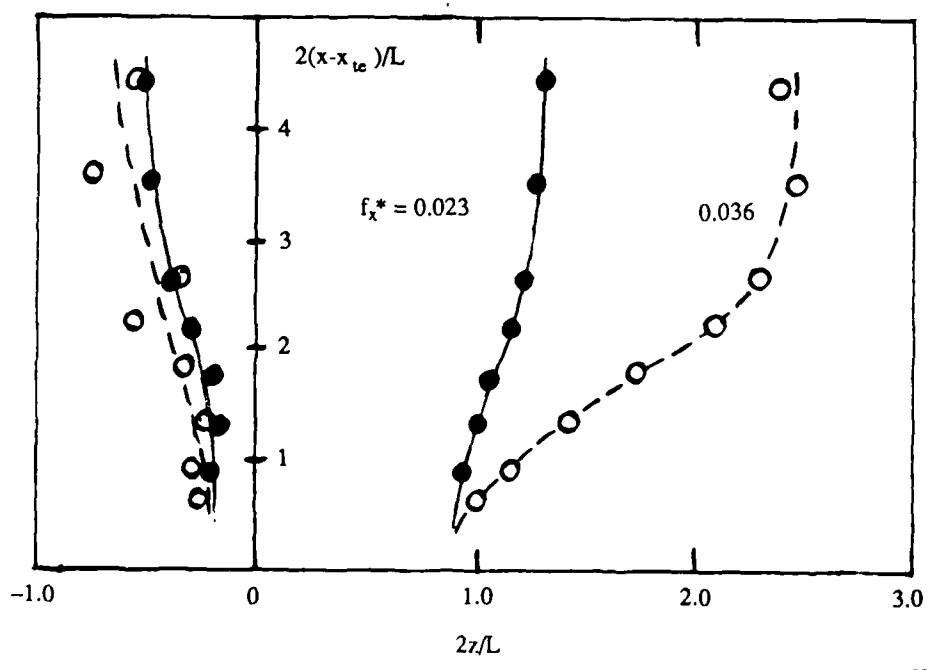


**Figure 11. Sensitivity of spreading rates to excitation frequency for swept-trailing-edge.**

### 3. EVOLUTION OF VORTEX SYSTEMS IN A CIRCULAR SHEAR LAYER

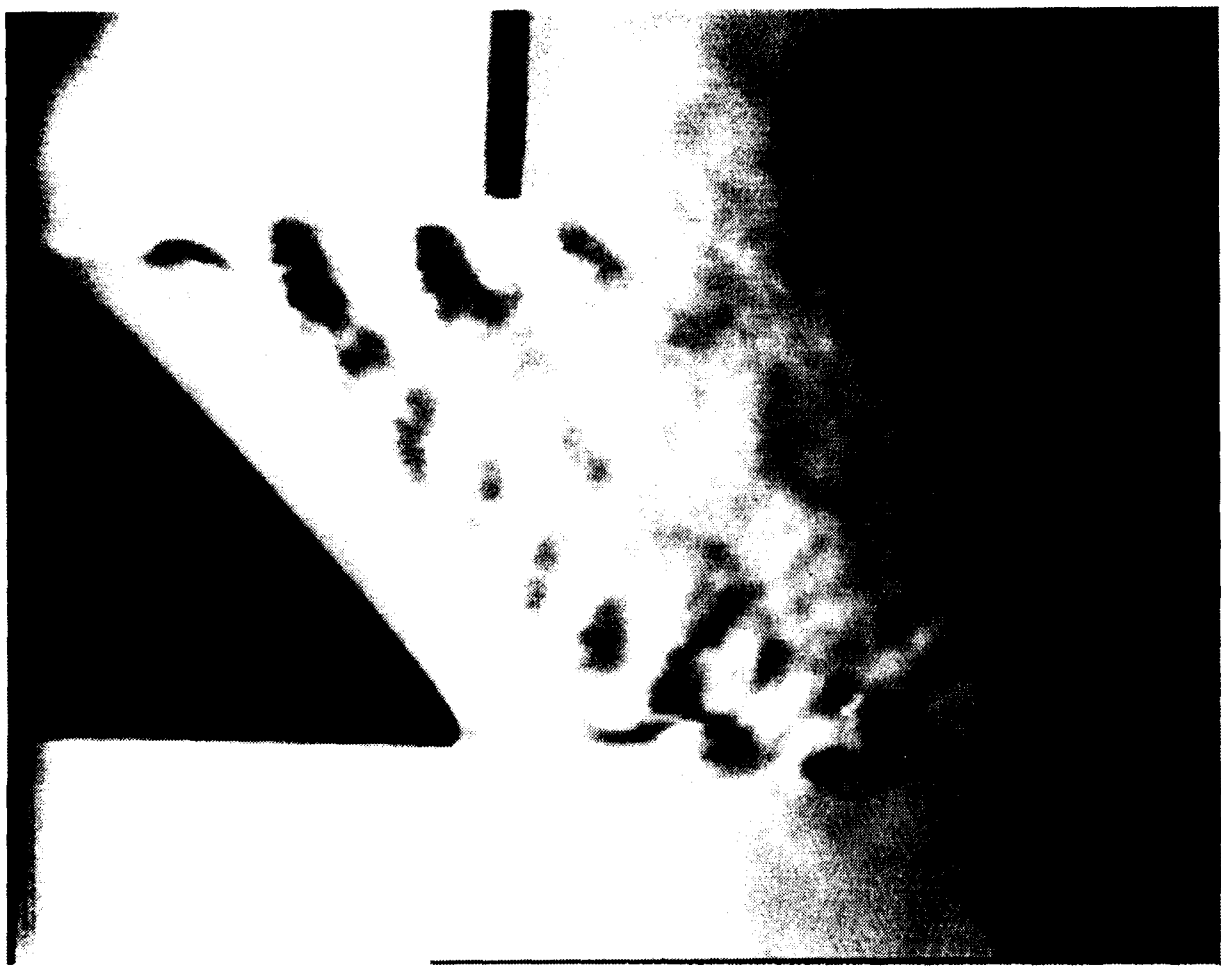
#### 3.1 Background

Vortex structures in circular shear layers often form as distinct axisymmetric vortex rings. Yet, various perturbations can quickly destroy the axisymmetry, leading to a highly three-dimensional structure. In this investigation, we have focused on the evolution of complex vortex structures in acoustically excited shear layers issuing from nozzles with slanted exits. We have also developed image-processing techniques that are useful for visually probing these flows.

In past work, funded under AFOSR Contract No. F49620-83-C-0048, we investigated the development of plumes from nonaxisymmetric nozzles (References 1 and 2). These included nozzles with slanted or stepped exits. In unexcited jets, the shear-layer instability-wave system was shown to undergo complex three-dimensional interactions which produce strong asymmetry in shear-layer spreading rates, and an overall net increase in jet spreading. Acoustic excitation was shown to produce an even wider range of shear-layer responses, as well as stronger asymmetry. The excited nonaxisymmetric jets have highly three-dimensional but strictly repetitive vortex systems, which are typified in Figure 12. In this case, the nozzle exit is inclined and the jet is acoustically excited at a subharmonic of the shear layer's initially most-amplified frequency.

However, it is not possible to determine the details of the interaction mechanism from these images since the schlieren process integrates the refraction of a light beam passing through the entire flowfield. Flow-visualization techniques not hampered by this inherent spatial integration were needed for characterizing the three-dimensional structure of vortex systems in these jets. If these techniques could also provide a quantitative description of the flow, one's understanding of the vortex interactions would be further enhanced.

In this second and final year of the contract, we added Fourier analysis to the image processing and performed detailed laser flow visualization to capture the evolution of streamwise vortices. The Fourier analysis allows one to separate the different spatial modes present in the vortex system. A



90-222-551

**Figure 12.** Schlieren image of complex shear-layer development in acoustically excited jet from inclined nozzle;  $U = 20$  m/s;  $f = 480$  Hz.

new two-color illumination scheme was developed for simultaneously viewing axial and transverse cross-sections of the shear layer. The quantitative description resulting from image processing is complemented by the detailed view of primary and secondary structures seen in the unprocessed cross-sections.

### 3.2 Approach

The flow system consisted of an electronically controlled blower, a settling chamber with honeycomb and screens, and a 6.25:1 or 23:1 contraction. At the end of the contraction, a constant diameter (63.5 or 25.4 mm) extension tube with a 45-degree inclined exit completed the asymmetric nozzle configuration. An indexing adaptor mounted the nozzle to the plenum and provided the capability to rotate the nozzle to an arbitrary azimuthal position. The quiet, stable flow produced by this system had a total fluctuating velocity of 0.15% at the nozzle exit.

The shear layer was made visible by injecting atomized seed material into the boundary layer immediately upstream of the extension tube and by illuminating the flow with either a laser or a strobe. An atomizer dispersed 1- $\mu\text{m}$ -diameter droplets of polyethylene glycol. Injecting the tracer nearly tangential to the main flow resulted in minimal disturbance to the jet.

A 20-W copper-vapor pulsed laser illuminated cross-sections of the shear layer. The optics system oriented the light sheet either parallel to the nozzle centerline or parallel to the slanted nozzle exit. With the light sheet passing through the centerline, rotating the nozzle illuminated axial cross-sections of the flow at different azimuthal angles. With the light sheet parallel to the nozzle exit, transverse cross-sections at different streamwise positions were obtained by traversing the light sheet. A single 30-ns pulse effectively illuminated an instantaneous cross-section. Phase-averaged views were produced by phase-locking the laser pulses to the acoustic excitation.

We developed a method for simultaneously illuminating both axial and transverse cross-sections. Taking advantage of the laser's emission of light at two wavelengths, 511 and 578 nm, we use a beam splitter to produce

separate green and yellow beams which are formed into axial and transverse light sheets (Figure 13). This approach has the advantages that only a single laser is required and that the two cross-sections can be easily distinguished by an observer or image processor because of the two colors.

The images were recorded on video tape with broadcast-quality video equipment. An Imaging Technologies ITI 200 image processor, hosted by a microVAX II minicomputer, performed the digitization and image processing. Images were also acquired directly by the image processor in real time.

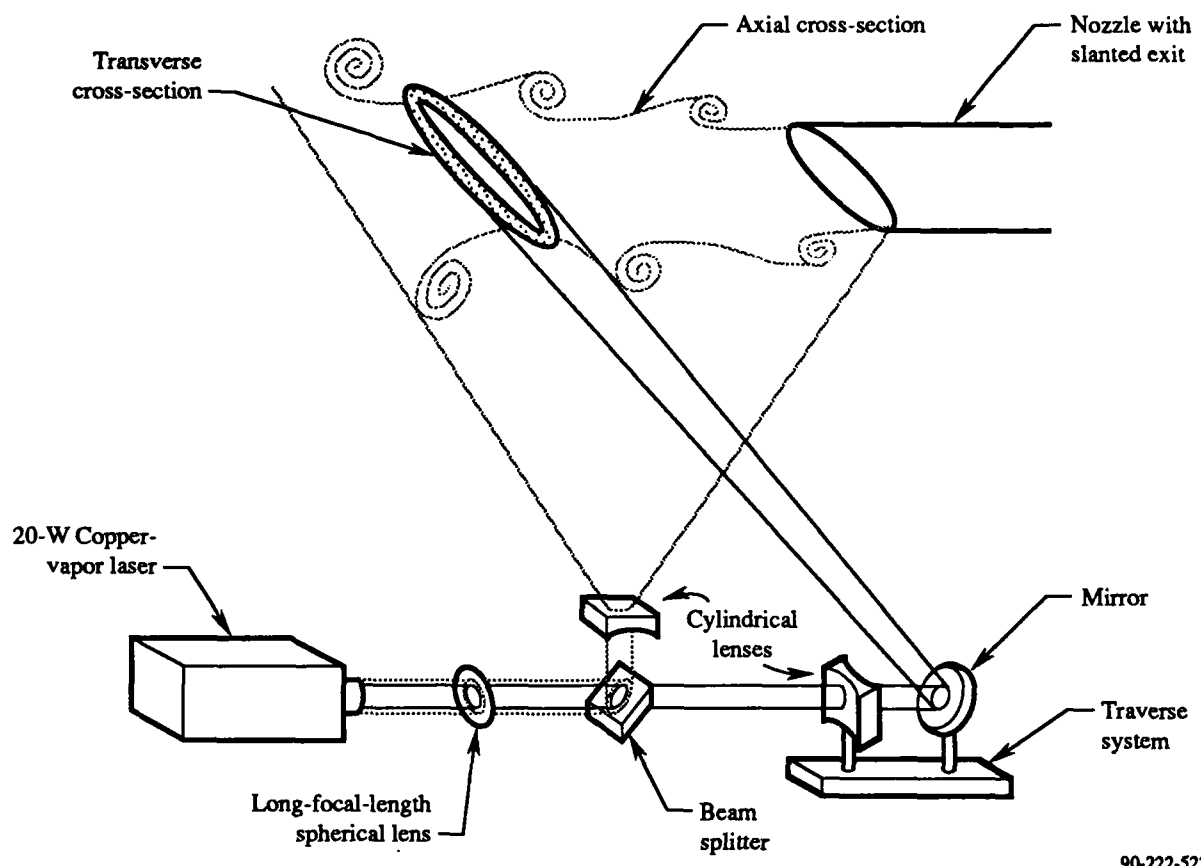
Acoustic excitation was generated by a compression driver coupled to the flow-system plenum. The excitation signal consisted of either a single frequency or of a composite signal whose frequency components corresponded to subharmonics of the shear layer's initially most amplified frequency. For the case of a jet exit velocity of 30 m/s, the most amplified frequency is approximately 3050 Hz. The acoustic excitation controlled the formation of vortices in the shear layer and provided a phase reference for conditional averaging.

### 3.3 Results and Discussion

We considered many cases over a wide range of excitation frequencies and amplitudes at jet exit velocities of 20 and 30 m/s. Strobe visualization provided an effective means for selecting the cases with the most distinctive features. The selected cases were investigated in detail by means of laser visualization and image processing. In this work the origin of the cylindrical coordinate system is the center of the nozzle exit, and a reference azimuth angle of 0 degrees corresponds to the most downstream edge of the nozzle.

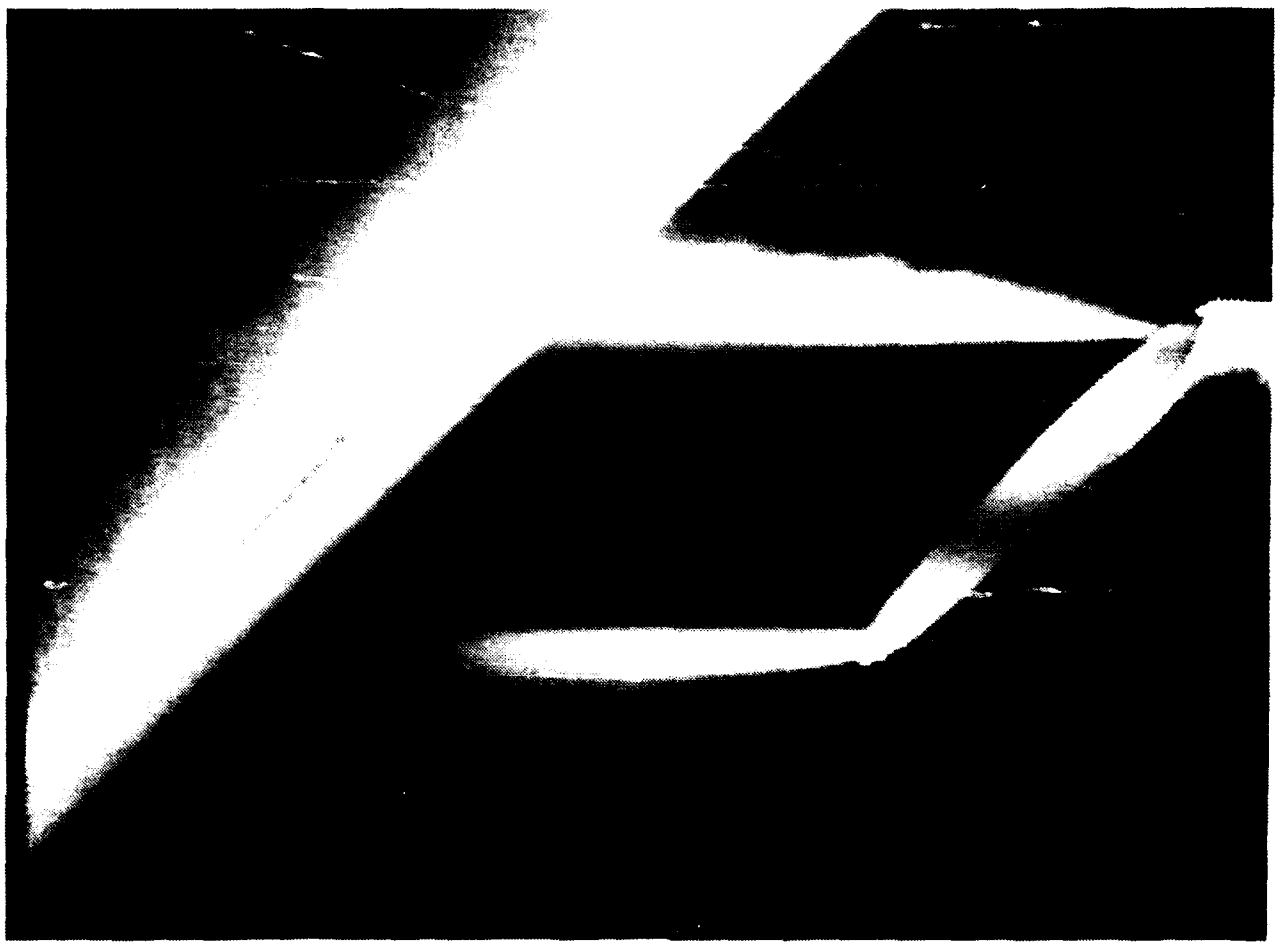
Simultaneous axial and transverse cross-sections of the natural jet are shown in Figure 14. This image was obtained by the two-color technique described in the previous section. Since the shear layer of an unexcited jet forms vortices in a quasi-random manner, no distinct structures are seen in this image, and the pulsed laser essentially functions as a continuous light source.

With the excited jet, one has a phase reference for the light source, making it possible to freeze the evolution of the vortex structures. Using



90-222-522

Figure 13. Schematic of simultaneous two-color flow-visualization system.



90-222-552

**Figure 14. Simultaneous axial and transverse cross-sections of unexcited jet;  $U = 20$  m/s.**

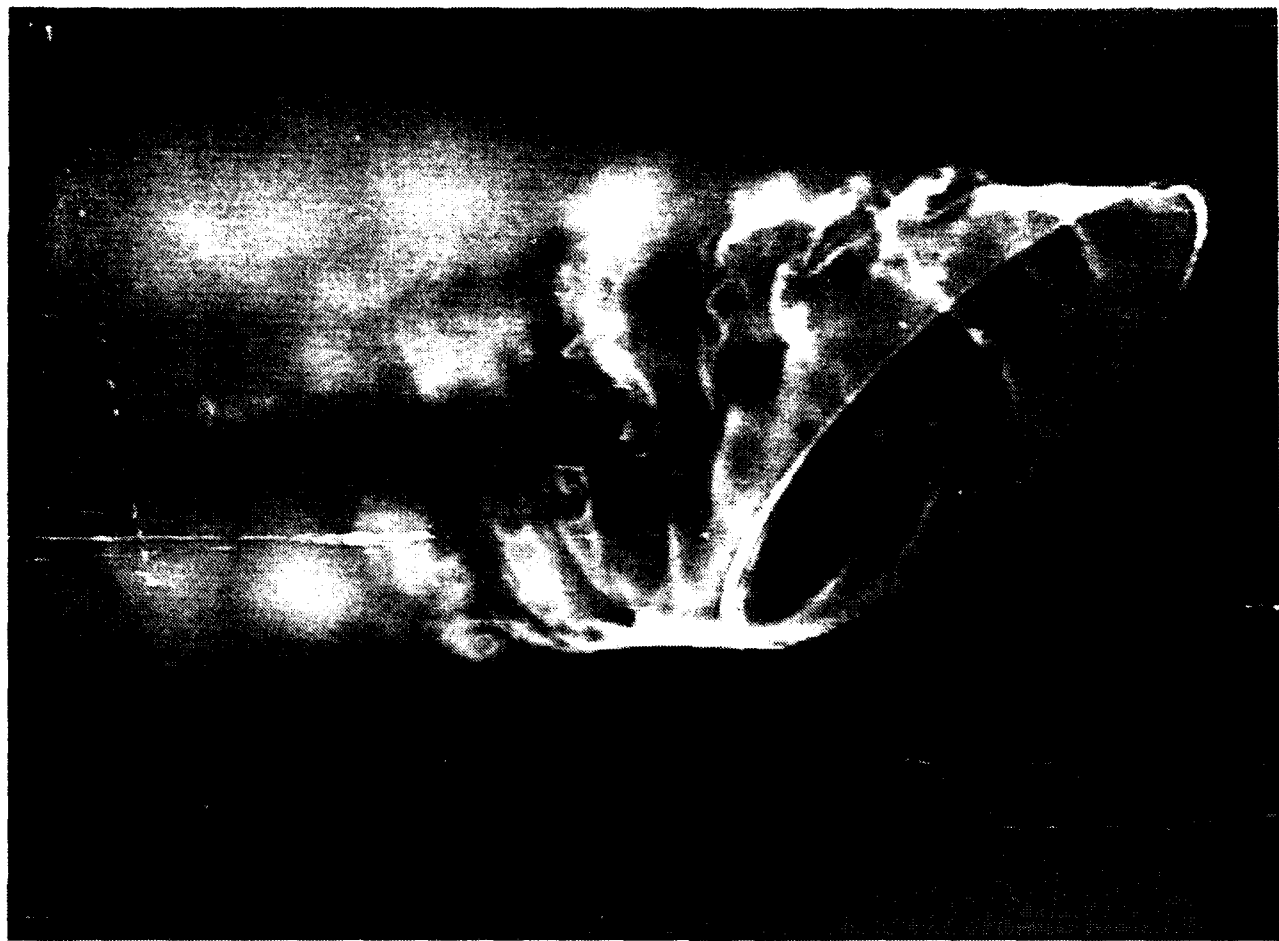
multiple pulses per image provides a phase average of the flow and highlights the features that are invariant at that particular phase. By increasing the light intensity relative to a single pulse, multiple pulses produce a brighter image that is easier to record.

Figure 15 is a strobe-illuminated image of an excited jet. The corresponding axial cross-sections at two different azimuthal orientations are shown in Figure 16. Transverse cross-sections at a series of streamwise positions are presented in Figure 17. In Figure 17, the light sheet is oriented parallel to the nozzle exit and the nozzle is oriented such that the leftmost section of the shear layer image corresponds to an azimuth angle of zero degrees. The streamwise position corresponds to the streamwise distance from the nozzle exit to the illuminated cross-section. The global view given by the strobe-illuminated image (Figure 15) provides the visual context for interpreting the detailed images seen in Figures 16 and 17.

The shear layer is initially symmetric and laminar (Figure 17a) but quickly becomes asymmetric as the vortex structures begin to form (Figure 17c). Since in this case the primary vortices are not oriented parallel to the light sheet, their cores are evident in the transverse cross-sections (Figure 17d). In Figure 17e, the shear layer appears symmetric across a horizontal plane but not across a vertical plane, indicating that the shear layer evolution does not simply depend on streamwise position.

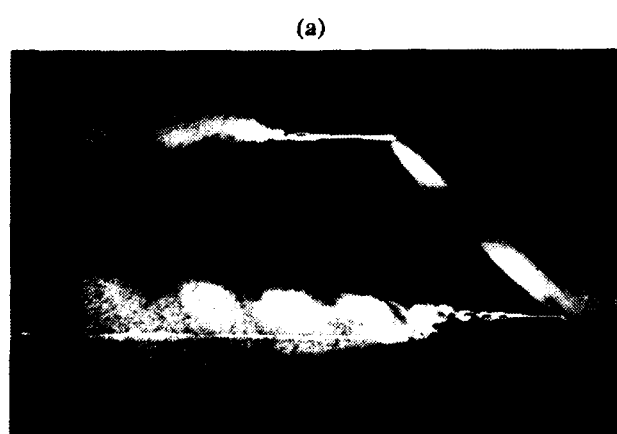
The initial shear layer characteristics are also affected by excitation amplitude. With zero excitation, the shear layer appears symmetric up to 15 mm downstream from the nozzle (Figure 18a). Increasing amplitude causes the vortices to form sooner (Figure 18b,c) since a higher initial disturbance amplitude requires less amplification by the shear layer prior to the onset of nonlinearity. With sufficient amplitude, the shear layer becomes nearly fully turbulent at this same streamwise position (Figure 18d).

While excitation amplitude affects the streamwise location of the onset of nonlinearity, excitation frequency alters the orientation of the primary vortex structures. For example, as shown in Figure 19, excitation at 972 Hz produces a system of vortices that are aligned perpendicular to the flow



90-222-553

**Figure 15.** Strobe-illuminated image of three dimensional vortex system in acoustically excited jet;  
 $U = 20 \text{ m/s}$ ;  $f = 486 \text{ Hz}$ .



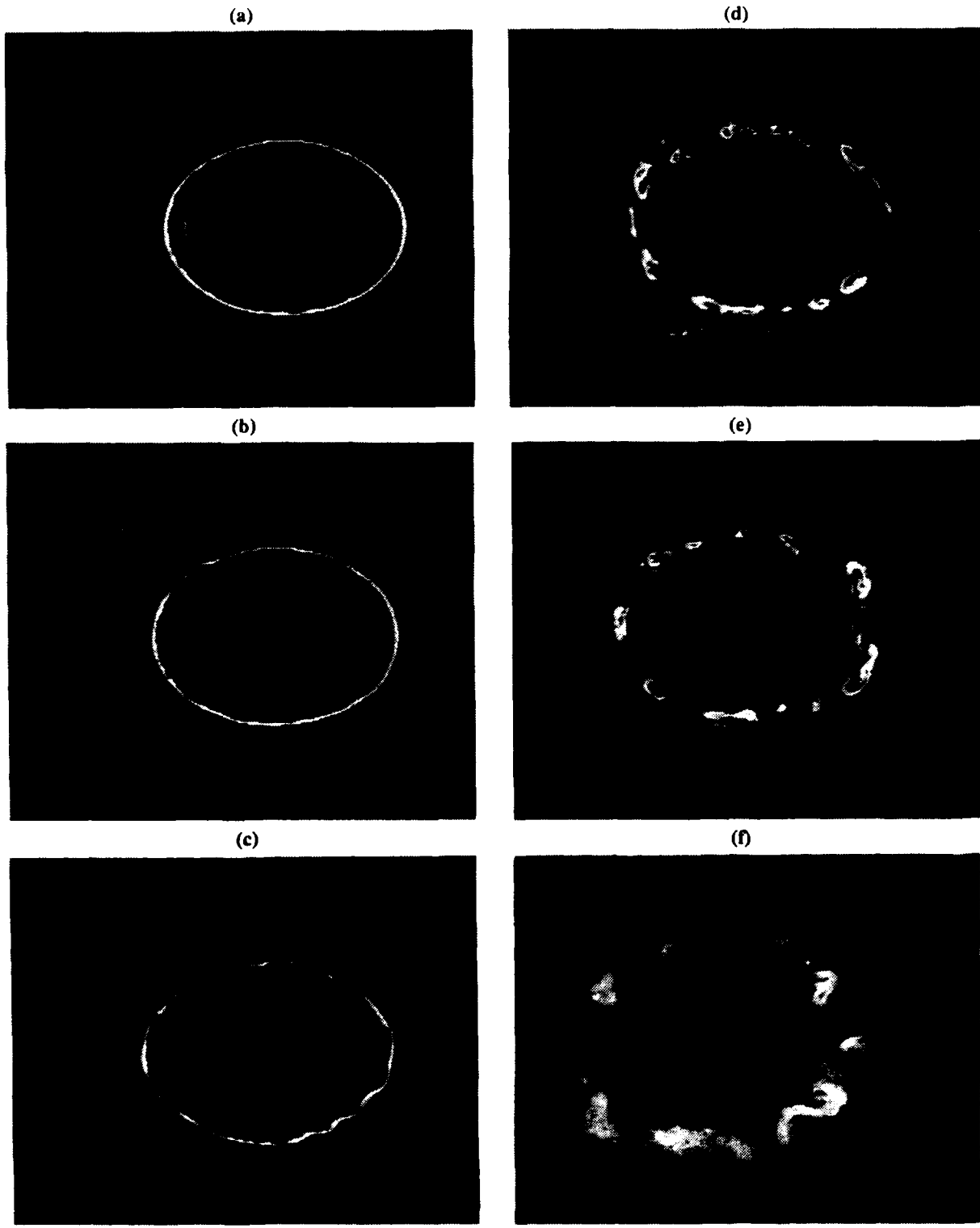
(a)

(b)



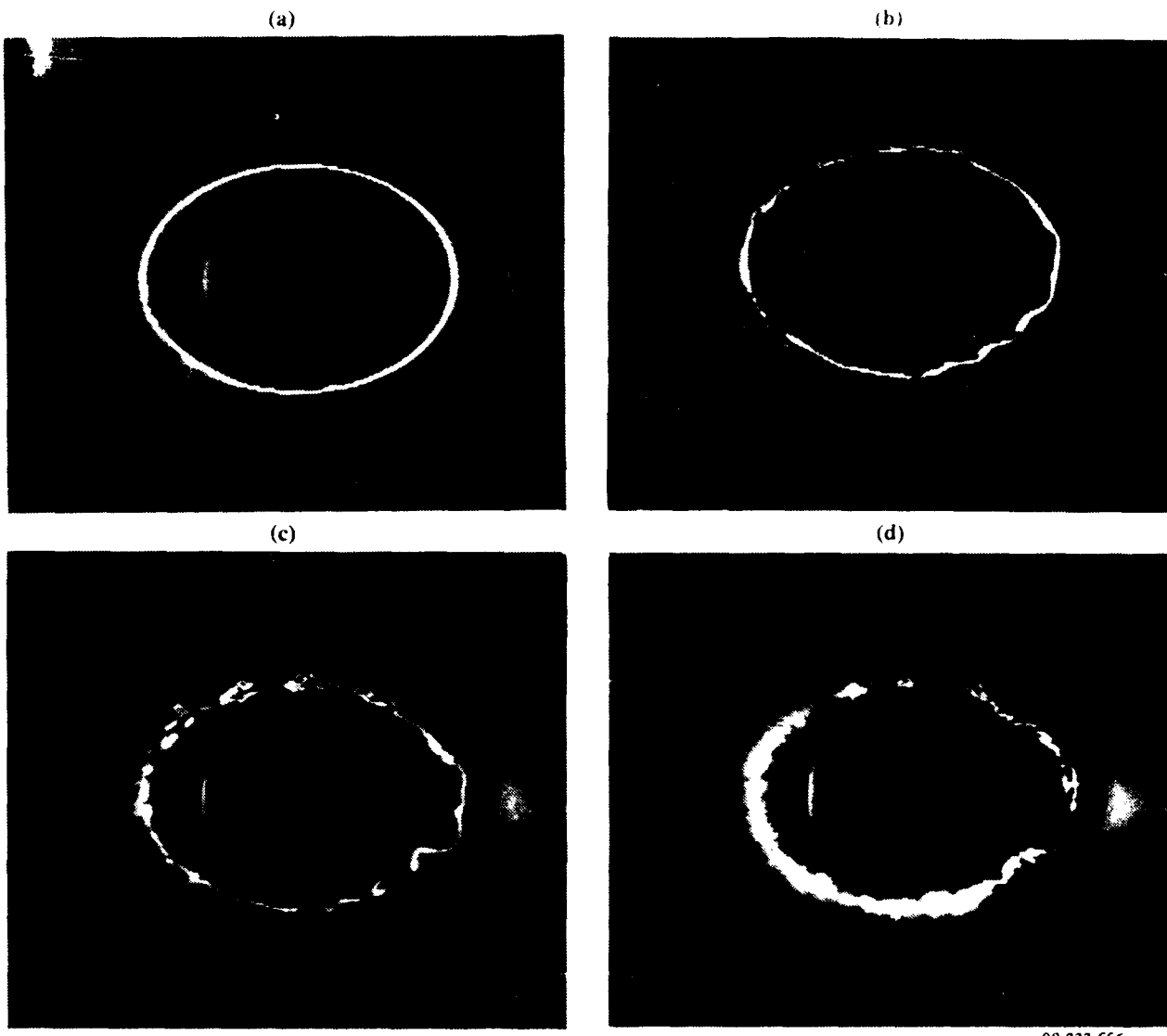
90-222-554

**Figure 16.** Axial cross sections of excited jet ( $f = 486 \text{ Hz}$ ) at azimuthal angles of (a) 0 and (b) 90 degrees.



90-222-555

**Figure 17. Transverse cross sections of excited jet ( $f = 486\text{Hz}$ ) at several streamwise positions  
(a) 5mm, (b) 10mm, (c) 15mm, (d) 20mm, (e) 25mm, (f) 40mm.**



90-222-556

**Figure 18. Influence of amplitude on shear layer instability ( $f = 486$  Hz;  $x = 15$  mm).**  
Normalized excitation amplitudes are (a) 0, (b) 2, (c) 5.3, and (d) 8.

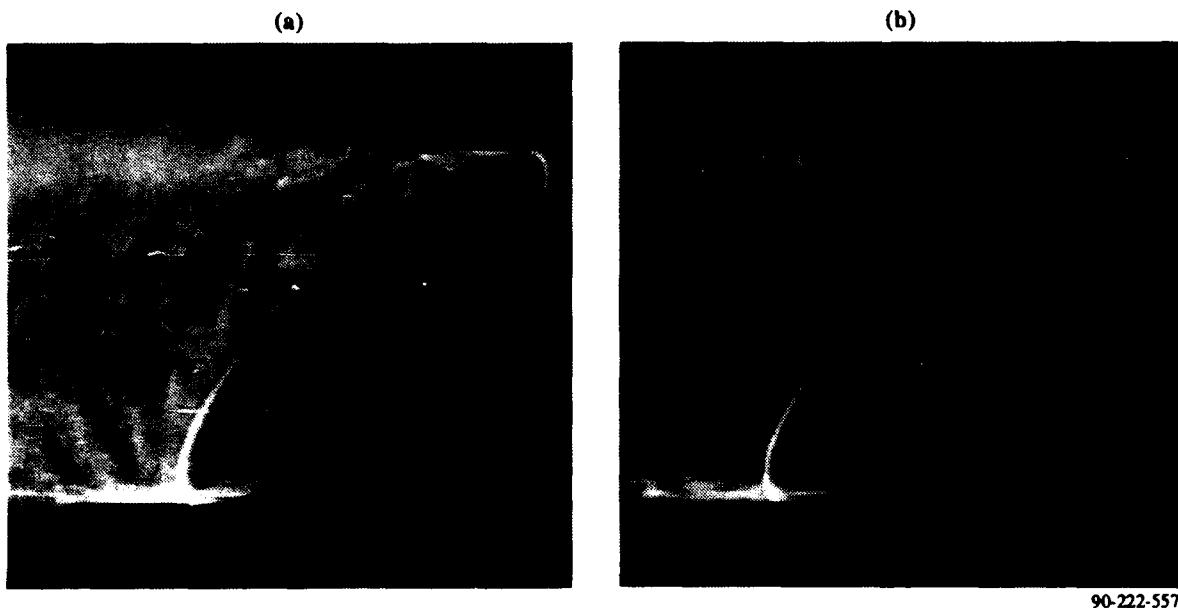


**Figure 19. Comparison of vortex orientation in excited jet for (a) 972-Hz and (b) 708-Hz excitation.**

direction, but excitation at 708 Hz results in vortices aligned nearly parallel to the nozzle exit. Results of excitation over a range of frequencies from 350 to 1400 Hz indicate that vortex orientations are similar over narrow subranges and over subranges that are harmonically related.

In the first year of work under this contract, we demonstrated that image processing could combine cross-sections of the jet at different azimuthal angles into a single view of an unwrapped shear layer (Reference 1). This involved integrating across the shear layer to quantify concentrations of vorticity and then mapping the cylindrical shear layer into a planar image. Such an image is shown in Figure 20a. The wavy bands correspond to vortex structures. The sinusoidal edge on the left side of the image is the nozzle edge. This case corresponds to the 25.4-mm-diameter nozzle, a jet velocity of 30 m/s, and excitation with frequency components of 1100 and 550 Hz.

This previous work was extended by adding modal decomposition in the Fourier domain. By computing a two-dimensional transform of the raw image (Figure 20a), the shear layer instability wave system can be decomposed into the  $m = 0$ , the positive  $m$ , and the negative  $m$  helical modes. If the Fourier components along the  $k_x$  axis are retained, a transform back to the image domain yields the axisymmetric modes (Figure 20b). The axisymmetric modes are relatively weak near the nozzle exit, and become stronger downstream as the initially nonaxisymmetric vortex system relaxes to an axisymmetric state. If all components except those along the  $k_x$  axis are retained, the positive and negative helical modes are retained (Figure 20c). The positive helical modes can be extracted by retaining only those components which lie above the  $k_x$  axis (Figure 20d). This decomposition shows that the helical modes decay rapidly in  $x$  and that the complex vortex interactions cannot be represented by the superposition of several low-order helical modes.

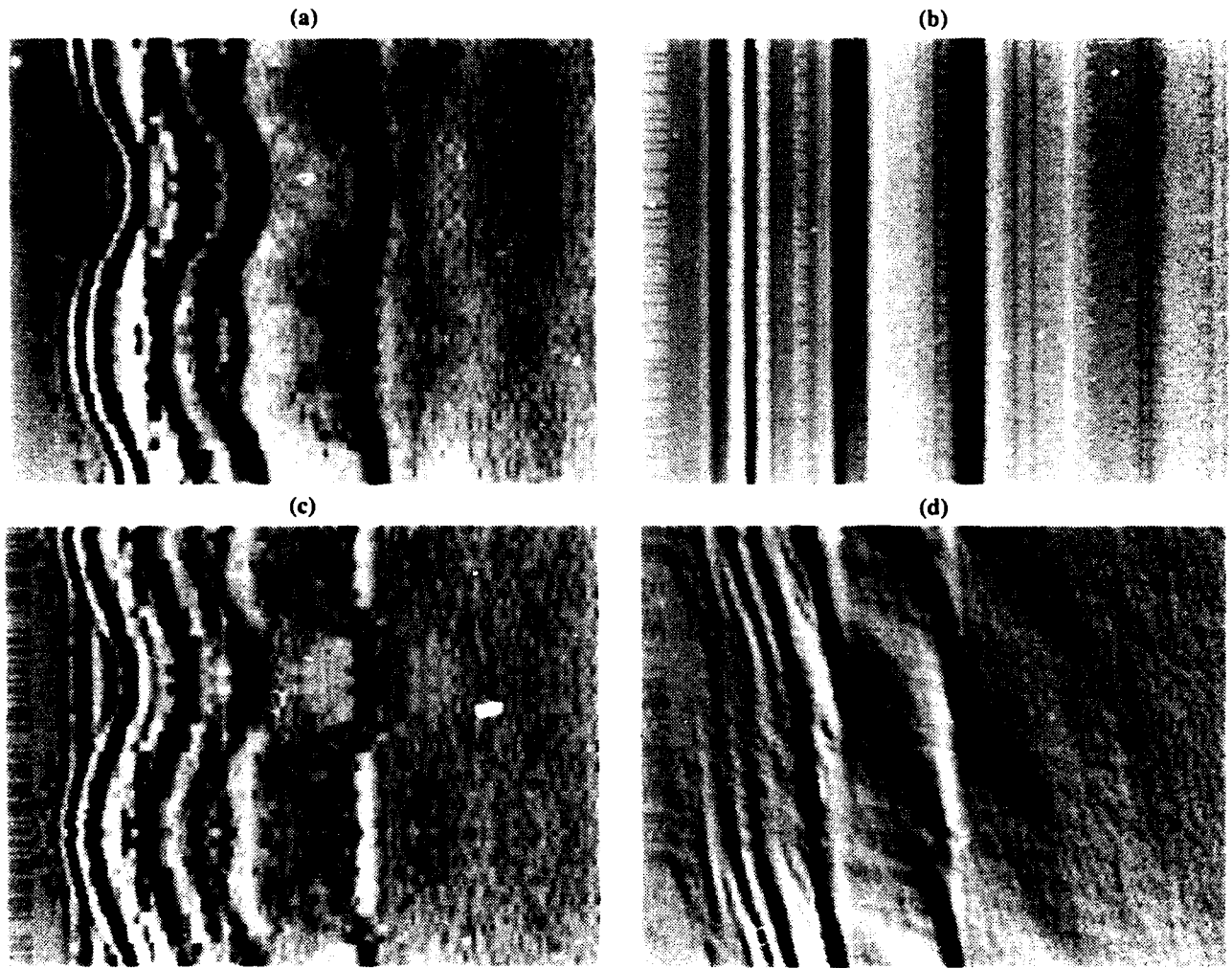


**Figure 20.** Unwrapped vortex lines: (a) raw image, (b) axisymmetric modes, (c) positive and negative helical modes, (d) positive helical modes.

#### 4. CONCLUSIONS

Wave systems of all orientations, from unswept to swept at the trailing-edge angle, have been observed in an excited, laminar, two-stream mixing layer behind a swept trailing edge. These wave systems are superposable, with no apparent interference effects. In all cases, constant-amplitude lines for growing waves remain approximately parallel to the local trailing edge. Wavelengths of the two primary wave systems (unswept and fully swept) are identical; the corresponding frequencies scale with the cosine of the sweep angle. Excitation at intermediate frequencies reveals a phase-jumping of finite-amplitude waves as sweep decreases. For the primary cases, mixing-layer growth differed significantly downstream of unswept and swept segments of the trailing edge.

Lateral spreading rates were moderately low for finite-span instability waves in shear layers behind swept and unswept trailing edges. The spreading rate was very sensitive to instability-wave excitation frequency, increasing with increasing frequency. It also increases with excitation amplitude and with increasing shear-layer velocity ratio. Behind a swept trailing edge, the spreading rate was asymmetrical, remarkably so at the higher excitation frequencies studied; the more rapid spreading was toward the trailing edge sweep direction. However, the lateral-spreading phenomenon was not, in general, sufficiently strong to produce the unswept instability waves observed in laminar shear layers behind swept separation edges. Hence the development of such unswept waves must involve the spanwise-nonuniform "crossover" phenomenon previously observed, or perhaps a nonlinear combination of the lateral-spreading and crossover phenomena.

Simultaneous axial- and transverse-cross-section laser sheet illumination of the flowfield of a slanted nozzle with a 45-degree inclined exit provided guidance for detailed studies of the development of shear layer growth. The frequency and amplitude of excitation strongly influenced the transition from a symmetric, laminar shear layer near the nozzle exit to an asymmetric, turbulent jet boundary geometry several jet exit diameters downstream of the exit. The choice of excitation frequency determined the orientation of the instability wave system to be either perpendicular to the

mean flow direction or parallel to the nozzle exit plane. Modal decomposition of digitized flow-visualization images showed axisymmetric and helical shear layer modes. The helical modes decayed rapidly, and the complex vortex interactions observed could not be represented as the superposition of low order helical modes.

## 5. REFERENCES

1. Wlezien, R. W. and Kibens, V., "Passive Control of Jets with Indeterminate Origins," AIAA J., Vol. 24, August 1986, pp. 1263-1270.
2. Kibens, V. and Wlezien, R. W., "Active Control of Jets from Indeterminate-Origin Nozzles," AIAA Paper 85-0542, 1985.
3. Kibens, V., Wlezien, R. W., Roos, F. W., and Kegelman, J. T., "Three-Dimensional Vortex Interactions," MDC Report QA005, annual technical report prepared for Air Force Office of Scientific Research, 1988.
4. Wlezien, R. W., "Quantitative Visualization of Acoustically Excited Jets," AIAA Paper 88-0499, 1988. Presented at the 26th Aerospace Sciences Meeting, Reno, Nevada, 11-14 January 1988.
5. Roos, F. W., Kegelman, J. T. and Kibens, V., "Two-Stream Mixing Layer From a Swept Trailing Edge," AIAA Paper 89-1022, 1989.
6. Roos, F. W. and Kegelman, J. T., "The Lateral Spreading of Finite-Span Instability Waves in a Laminar Mixing Layer," AIAA Paper 90-1532, 1990.

## 6. PUBLICATIONS AND PRESENTATIONS

The following publications and presentations originated from the present contract during the period of performance covered by this report.

1. Wlezien, R. W., "Quantitative Visualization of Acoustically Excited Jets," AIAA Paper 88-0499, 1988. Presented at the 26th Aerospace Sciences Meeting, Reno, Nevada, 11-14 January 1988.
2. Roos, F. W., Kegelman, J. T., and Kibens, V., "Two-Stream Mixing Layer From a Swept Trailing Edge," AIAA Paper 89-1022, 1989. Presented at the AIAA 2nd Shear Flow Control Conference, Tempe, Arizona, 13-16 March 1989.
3. Parekh, D. E. and Collis, S. S., "Evolution of Complex Vortex Systems in a Perturbed Circular Shear Layer". Presented at the 42nd Annual Meeting of the American Physical Society Division of Fluid Dynamics, Palo Alto, California, 19-22 November 1989.
4. Roos, F. W. and Kegelman, J. T., "The Lateral Spreading of Finite-Span Instability Waves in a Free Shear Layer." Presented at the 42nd Annual Meeting of the American Physical Society Division of Fluid Dynamics, Palo Alto, California, 19-22 November 1989.
5. Roos, F. W. and Kegelman, J. T., "The Lateral Spreading of Finite-Span Instability Waves in a Laminar Mixing Layer," AIAA Paper 90-1532, 1990. Presented at the AIAA 21st Fluid Dynamics, Plasmadynamics and Lasers Conference, Seattle, Washington 18-20 June 1990.